Experimental investigation of an electrostatic adhesion device used for metal/polymer granular mixture sorting

Hamza Louati, Noureddine Zouzou, Amar Tilmatine, Ayyoub Zouaghi, Rabah Ouiddir

Version of Record: https://www.sciencedirect.com/science/article/pii/S003259102100543X
Manuscript_e1d62a4e6c4e3f143fbff8940a079a15

Experimental investigation of an electrostatic adhesion device used for metal/polymer granular mixture sorting

H. Louati[1,2,3], N. Zouzou[1], A. Tilmatine[2,3], A. Zouaghi[4], R. Ouiddir[2,3]

[1] Institut Pprime, CNRS, Université de Poitiers, ISAE-ENSMA, F-86962 Futuroscope, France

[2] LGEO Laboratory, University of Science and Technology-MB, Oran, Algeria

[3] APELEC Laboratory, University Djillali Liabès, Sidi-Bel-Abbès, Algeria

[4] Univ Lyon, Ecole Centrale de Lyon, INSA Lyon, Université Lyon 1, CNRS, Ampère, UMR5005, 69130 Ecully, France

Abstract

Electrostatic adhesion (EA) technique have been used recently for the electrostatic sorting of metal/polymer granular material mixture. The action seat on the materials is an EA actuator composed of an interposed electrodes network covered by a dielectric barrier and powered by polyphase voltages. The sorting principle consists of attaching the metal particles by EA, and of moving the polymer particles larger than 500 µm, mainly by gravity and vibration. The purpose of this paper is to optimize the EA mechanism for electrostatic sorting. The first part consists of evaluating the behavior of materials (Cu, PE, and PVC) on the EA actuator surface using a 180°-rotating system. The results showed that the metal attaches to the actuator surface while the polymer does not; they also indicate the optimal factors contributing to the adhesion process. In the second part related to sorting application, the granular materials behavior and the influencing factors are explored in an inclined vibrating system to process a Cu/PVC mixture. For an inclination of 10°, Cu recovery on the actuator exceeds 98% with a purity of about 99%.

Keywords: Electrostatic adhesion actuator; Metal/polymer granular mixture; Electrical and geometrical parameters optimization; Electrostatic sorting performance.

1. Introduction

The industry of electrical and electronic equipment (EEE) is a fast-developing sector with continuous changes in the equipment features, the treated materials, the used techniques and their capabilities. This development results in an increasing trend of EEE production and sales, which is contrasted with decreasing the equipment use lifetime [1]. The waste electrical and electronic equipment (WEEE) is one of the fastest growing waste streams in the world [2]. WEEE represents a large and increasingly diverse waste, with an estimated global arising of over 40 Mt/year, and is a resource-rich stream of increasingly valuable materials that must be carefully managed [3]. Appropriate treatment and disposal of WEEE are indispensable for the development of a circular economy in order to reduce the impact on the environment. Since inappropriate treatment of WEEE may cause severe pollution, environmentally friendly recycling has been heavily promoted by laws and regulations in recent years [4].

Many studies have been carried out on the recovery of granular metal/polymer mixtures from industrial WEEE including electric cables [5]. The most used devices are the vibrating densimetric tables [6-9], and the electrostatic separators [10-17]. The densimetric tables are based on the difference between the density values of metal and plastic granules, while the operating principle of the electrostatic corona discharge separators is based on the difference between their electrical conductivity [5,10].

Among the electrostatic solutions for conductive and non-conductive materials sorting, one can find the roll-type separator and the plat-type separator [5], [10]. The major disadvantage of these systems is the use of a corona discharge, that introduces additional electric power consumption and risks for the equipment and for the operator due to the applied voltage level. Moreover, the multitude of parameters make it difficult to control the particles trajectory.

Among the electrostatic sorting solutions, there is the EA technology which does not require very high voltages and does not need an external active electrode for the generation of corona discharge to sort the granular materials. A drum-shaped electrostatic sorting device (ESD), with an inter-digitated

electrode configuration, has been recently developed by our research teams for the separating of metal/plastic granules sized between 1 and 10 mm [17]. The principle function of this device is to supply the electrode system with polyphase voltages in order to generate an electric field allowing the manipulation of the particles mixtures. This involves capturing the conductive particles on the drum surface under the effect of the EA force and then collecting them in the corresponding box using a squeegee, and acting on the insulating particles under the effect of centrifugal and gravitational forces to collect them in the dedicated box.

The configuration of parallel electrodes, arranged on a dielectric surface and supplied with polyphase alternating voltages, is used in travelling wave conveyor (TWC) and EA actuator applications [18-19]. The TWC is used for the manipulation of different type of particles with a typical size less than 500 µm [20] such as aerosols [21] and toner particles [22], and also for the separation and displacement of insulating particles [23-28]. Recently, many research works have investigated the use of this system for dust removal from solar panels in both atmospheric and space conditions [29]. The results are very promising. In fact, supplying the TWC with AC voltages generate a non-uniform electric field which causes the motion of particles under the action of electrostatic forces [20]. When the system is energized with two-phase voltage, electric potential standing waves occur. However, traveling wave effect appears when using at least three-phase electrode configurations [30].

EA technology extends the applicability of electrically controllable adhesion to many materials and applications [31], including robotic adhesion mechanism [32], mechanical and electrical interconnections [33], and effectors for gripping advanced composites and fibrous materials [34-35]. The attachment is manifested by EA force which appears when the two surfaces are subjected to the action of an electric field, generated by two layers of electric charges with opposite sign [36-37]. The electric field, which is set up by the applied voltages between the electrodes (Fig. 1), can polarize or induce opposite charges on the substrate surface and thus causing electrostatic adhesion force between the interdigitized electrodes and the surface of substrate materials [38-40]. The normal direction of the electrostatic adhesion force F_{adhy} acting on the material is given by the following formula [41-45] :

$$F_{adhy} = \frac{1}{2}\varepsilon l \int_{x_0}^{x_0+L} \left(E_y^2 - E_x^2\right) dx \quad (1)$$

Where E_x and E_y are the electric field components, ε the dielectric permittivity of the medium, x_0 the initial position of integration, L and l represent the length and width of material, respectively.

The aim of this work is to experimentally investigate the electrical and geometrical parameters allowing the optimization of the EA mechanism required in the electrostatic sorting of metal/polymer materials mixture. The devices used in this investigation, that act on particles of average size between 0.5 mm and 5 mm, consist of interdigitized electrodes of planar shape placed on two systems. The first one is a 180° rotating configuration, that allows of evaluating the behavior of each material (metal or polymer) on the surface of the EA actuator. The second one is an inclined vibrating system, that allows the investigation of the performance of a Cu/PVC mixture sorting using an EA actuator.

2. Optimization of the electrostatic adhesion actuators

2.1. Experimental configuration and protocols

The EA actuators are the key part of the experimental setup, as they allow the granular materials handling. These devices are made of a network of interdigitized electrodes placed on a dielectric support, covered by an insulating film and powered by polyphase voltages. The actuators studied in this work are illustrated schematically in Fig. 2. The first one is energized with two-phase voltages (Fig. 2.a), and the second one is supplied with three-phase voltages (Fig. 2.b). Each of them is made of a 90×100 mm² printed circuit board (PCB).

The electrode width w and spacing g for the used actuators are given in Table 1. The surface of the EA actuators is covered with a 27 µm-thick Kapton adhesive film (dielectric constant of about 3.3). The insulating adhesive film is used to prevent breakdown sparks between the electrodes, especially when handling conductive particles.

The first experimental setup used in this investigation, called 180° rotating system, is illustrated schematically in Fig. 3.a. It allows measuring the mass of particles attached to an EA actuator due to

electrostatic adhesion force. The EA actuator is fixed on a rotating support with angles comprised between 0 and 180°. Fig. 3.b shows a typical behavior of the copper samples when the applied voltage is turned on. Even in vertical position (angle of 90°), Cu particles can remain attached to the surface due to electro-adhesion force. By changing the electrical and geometrical parameters of the actuators and the properties of the particles, it is possible to find the optimal experimental conditions to be used for the electrostatic sorting of a mixture of particles with different electrical properties.

Each phase of the EA actuator fixed on the 180° rotating system is supplied through a HV connector with a voltage amplifier (Trek, model 2220, ±2 kV, ±20 mA). The HV amplifiers (up to four units) are controlled by a digital function generator (TTi, model TGA1240, 16 MHz). A digital pulse generator (Stanford, Model DG645) is used as a synchronizer for triggering the electrical signals supplied to the actuator. The 180° rotating system can provide: two or three phases, sine or square high voltage signals; with an amplitude up to 2 kV and a frequency up to 10 kHz. The electrical signals of the applied voltages are visualized using a digital oscilloscope (Lecroy, model 424, 200 MHz, 2 GS/s).

All the experiments were performed in stable climatic conditions of temperature (23 ± 3 °C) and relative humidity (45- 55%), which is the relative humidity of the experiment room measured during the study. The impact of moisture on separation efficiency is not studied in the present work. The measurements were repeated three times and the average value was obtained for plotting.

The electrical and geometrical parameters that have been analyzed in this work are: the applied voltage V, the voltage waveform, the frequency f, the duty cycle and the phase shift for a square signal, and also the ratio K between spacing and electrode width.

The experiments were carried out using a sample of metal (Cu) and polymer (PE or PVC) particles obtained after granulation of electric cables, for particle sizes that vary between 0.5 and 5 mm (Fig.). The optimal factors effect on the shape and the size of the particles is investigated in other work that will be published in others paper, so they are not considered in this work. The electrical conductivity of copper wastes wires is 59.98 10^6 S/m with a density of 8700 kg/m^3. The relative dielectric

permittivity of PE and PVC is 2.3 and 2.9, respectively. The density of each of these two polymers is equivalent to 1760 kg/m^3 and 930 kg/m^3, respectively. These values were obtained from data sheets of COMSOL Multiphysics software library. The materials were deposited on the EA actuator in the shape of a monolayer. The mass of each material used for the experiments in the 180 ° rotating system is M_{tot} = 2 g. The behavior of other materials is currently being analyzed and will be the subject of another publication.

The goal of the study using the rotating system is to determine the behavior of each material (Cu, PE or PVC) separately under the action of the parameters mentioned above. The principle is to deposit a monolayer of 2 g of Cu, PE or PVC on the surface of the actuator attached to the 180° rotating system. Initially set to the horizontal position, the actuator is then turned at an angle of 180°. A quantity of the product remains stuck, while the rest falls into the collection box placed on an electronic balance (Kern, model 440). The idea was to control the particles mainly under the effect of EA forces and gravity. The performance is interpreted by the adhesion rate of each material deduced from the mass to be recovered. The adhesion rate of the retained material R_r is calculated as follows:

$$R_r(\%) = (M_R/M_{tot}) \times 100 \quad (2)$$

Where M_R is the mass of material (Cu, PE or PVC) retained on the EA actuator, M_{tot} the total mass of the material deposited on the EA actuator given by:

$$M_{tot} = M_R + M_F \quad (3)$$

With M_F the mass of the material that has fallen into the collection box.

The measurement errors caused by the uncertainties of the electronic balance and the losses of materials in the electro-adhesive system have been estimated at 3% and neglected.

2.2. Results of the adhesion in rotating system

This part describes the results obtained with the experimental device illustrated in Fig. 3, in order to determine the behavior of metal and polymer particles separately. The EA actuator used to analyze the

influence of the electrical parameters on the materials is the reference one ($g = w = 1\,mm$) for the two-phase and three-phase configurations.

2.2.1. Case of conductive particles

The following results were obtained by using the 180° rotating device to determine the interaction of Cu with EA actuator as a function of applied voltage, signal waveform, frequency, duty cycle and phase shift, and the ratio between spacing and the electrode width. The influence of the signal waveforms is introduced in the sub-sections dedicated to the effect of the applied voltage and the frequency.

A. Voltage effect

Fig. 5 shows the variation in the Cu adhesion rate as a function of the applied voltage for sine and square signals at 300 Hz. As expected, the adhesion of Cu increases with the applied voltage considering that the adhesion force is proportional to the square of the applied electric field [41].

The adhesion rate can reach 97% for the best case. The applied voltage magnitude for which the adhesion becomes effective is lower in the case of square signal (about 100 V for square signal against 200 V for the sine signal). For applied voltages in the range between 200 V and 600 V, the adhesion of Cu for the square signal is greater than for the sinusoidal signal. This is explained by the potential difference ΔV between two adjacent electrodes. For the square signal, ΔV remains constant, except during the brief moment of switching, then the instantaneous electric field in most of the time is higher, unlike the case of the sine voltage which changes over time. The typical experimental voltage waveforms used for the energization of the actuator are shown in Fig. 6.

B. Frequency effect

Fig. 7 illustrates the variation of the Cu adhesion rate as function of the frequency for a sinusoidal signal, at different applied voltage values. In this case, the copper adhesion rate increases with the frequency up to 300 Hz whatever the applied voltage value, then it decreases for higher frequencies. The frequency range for which the adhesion rate is broader is obtained at high applied voltage.

The results associated to the square signal case are shown in Fig. 8. The curve's shape is different from that obtained with the sine signal. The adhesion rate of Cu particles is enhanced at low frequency using the square signal. Thus, the curve dynamics are less steep between 0.1 Hz and 300 Hz, in particular for high applied voltages.

In both sine and square signals, the decrease of adhesion rate observed at high frequency is probably due to the limited value of the slew rate of the power supply. Thus, the sine high voltage signal becomes almost triangular, while the square HV signal looks like a trapezoidal waveform, this slew rate increase as a function of the frequency and approaches the maximum of the amplifier (100 V/μsec). Consequently, the duration time required for polarity changes increases with respect to period, which reduces the attachment effect of copper particles.

C. Number of phases effect

Fig. 9 presents the evolution of the adhesion rate as a function of the applied voltage with different voltage waveforms for both two-phase and three-phase EA actuator. The number of electrode phases has an important effect on the electric field distribution above the electrodes, and the existence of a significant progressive electric potential waves. However, the results of the adhesion rate of Cu using two-phase actuator are better in particular using square signal. In this particular case, the potential difference between two successive electrodes is at highest level for nearly the overall period of the alternating signals.

The typical experimental voltage waveforms used for the energization of the three-phase actuator are shown in Fig. 10. In the case of the three-phase square voltage, a Cu particle placed between two electrodes undergoes a zero-potential difference during a long time period (for instance T/6 when the values of the applied voltages are maximum); this time interval favors the detachment of conductive particles. The same is true for the case of a sinusoidal voltage when the two signals tend to cross over time as shown in Fig. 10.

D. Duty cycle and the phase shift effects

After demonstrating that the adhesion rate of Cu is optimal for the two-phase square configuration, it is interesting to analyze the effect of the duty cycle and phase shift on the adhesion rate. The obtained results are illustrated in Fig. 11 and Fig. 12. Obviously, the efficiency of the actuator is maximum for the phase shift of 180°, which corresponds to the value of 100% of duty cycle. However, it is possible to maintain that high level for a wide range of duty cycles (70 % - 100 %) and phase shifts (120°-180°).

It should be noted that, more the width of the applied voltage plateau tends to occupy the time interval in a half period, more the efficiency is maximum. For the phase shift, it can be seen that when the two voltages are in phase (0°) the efficiency is zero, on the other hand when they tend to oppose each other (180°), the adhesion becomes maximum.

E. Electrode gap to width ratio effect

The influence of electrode geometry on the Cu adhesion rate has been studied using six EA actuators, with the dimensions indicated in Table 1. In order to ensure the comparison in the same conditions, the electrodes were supplied by voltages leading to the same reduced field Er equivalent to 1000 V/mm (for instance, V= 1000 V and g = 1 mm). The variation of the adhesion rate as a function of the ratio between electrode width and gap spacing is shown in Fig. 13. Whatever the frequency level, the adhesion rate increases with g/w ratio, reaches a maximum, then decreases for higher electrode gap/width ratio. The optimal ratio is between 0.5 and 1. This result is linked to Cu particle size. For high electrode width (low g/w ratio), some Cu particles could be entirely positioned on an electrode as shown in the Fig. 14, therefore no electro adhesion force is created. For high g/w ratio, some copper particles could be positioned in the interelectrode space, which reduces accumulation of charge under the particles.

2.2.2. Case of insulating particles

The previous sections indicate that metal particles could be attracted efficiently in the case of two-phase square signal. In this section, we will study the action of an EA actuator on polymer particles, in

order to proceed to the electrostatic sorting of the two materials. Fig. 15 shows the evolution of adhesion rate of PE and PVC particles as a function of frequency for a square signal. The results clearly show that the PE and PVC do not adhere to the surface of the EA actuator whatever the value of the frequency and the applied voltage, within the studied range. The electrical conductivity of the polymer is very low; therefore, the electrostatic adhesion force is also low compared to other mechanical forces, this favors the non-adhesion of this material. Under the same conditions, the EA of Cu particles is effective. The mobility of charge in the metal allows the EA force to predominate the gravity force. These results are very interesting since they open the perspective for the development of electrostatic separation process of metal/polymer mixture.

3. Application of electrostatic adhesion for mixture sorting

3.1. Experimental configuration and protocol

In this section, a specific experimental setup is used to evaluate the performance of electrostatic sorting of a metal/polymer mixture, as illustrated schematically in Fig. 16.a. The electric system is the same used in section 2. The actuator corresponds to the geometry with ratio between gap spacing and electrode width $g/w = 0.5$. The EA actuator is fixed at the end of a vibrating feeder. The angle of the actuator with respect to the horizontal plane varies between 0 and 70°. When the system is turned on, the particles move along the vibrating plate of the feeder and fall on the EA actuator. Depending on the experimental conditions, a fraction of the mixture remains on the actuator and the other part is collected in a box. The mass of the collected particles, both on the actuator and the collecting box, are measured, then the purity of the products is evaluated. Fig. 16.b shows a typical photography of the sorting system under operation to separate a mixture composed of Cu and PVC samples.

The objective in this case is to move on to the application of the EA actuator in electrostatic separation. The principle is to act on the mixture at the same time. Thus, a material mixture of 4 g comprising 50% Cu and 50% PVC is put evenly on the vibratory feeder. Then, with a controlled flow, the sample is delivered to the vibrating EA actuator. The flow rate of the particle delivery has been controlled to have a homogeneous and monolayer distribution on the EA actuator fixed in an inclined

position. Some of the material adheres to the actuator surface by EA force, and another amount falls under the effect of mechanical vibration. The separation efficiency was estimated using the following formulas:

$$R_{Cu}(\%) = \left(\frac{M_{Cu}}{M_{\mathrm{IntCu}}}\right) \times 100 \quad (4)$$

$$P_{Cu}(\%) = \left(\frac{M_{Cu}}{M_{EAA}}\right) \times 100 \quad (5)$$

Where,

R_{Cu} and P_{Cu} are the recovery and the purity of Cu on the EA actuator, respectively.

M_{Cu} and M_{IntCu} are the mass of Cu particles, on the EA actuator and initially deposited on the vibro-transporter, respectively.

M_{EAA} is the total mass of both Cu and PVC particles remaining on the EA actuator.

The recovery and purity rates of PVC particles collected in the box, R_{PVC} and P_{PVC}, respectively were calculated as follows:

$$R_{PVC}(\%) = \left(\frac{M_{PVC}}{M_{\mathrm{IntPVC}}}\right) \times 100 \quad (6)$$

$$P_{PVC}(\%) = \left(\frac{M_{PVC}}{M_{box}}\right) \times 100 \quad (7)$$

Where,

M_{PVC} and M_{IntPVC} are the mass of PVC particles collected in the box and initially deposited on the vibro-transporter, respectively.

M_{box} is the total mass of both Cu and PVC particles collected in the box.

To calculate the recovery and purity rate of each material after each separation operation, the masses of Cu and PVC remaining on the plate and the collection box were deduced from a second separation of these materials by exploiting the optimal inclination corresponding to an angle of 10°.

3.2. Separation results using inclined vibrating process

This section summarizes the results obtained with the experimental setup to understand the action of the EA actuator on the combination of materials, necessarily for the separation process.

Fig. 17 show the evolution of the Cu recovery and purity as a function of the inclination angle for constant values of the applied voltage and the frequency (400 V, 300 Hz), on the actuator. With increasing the inclination, the recovery of Cu decreases on the actuator, and increases by the same ratio in the collection box. It is noticed that the purity of the Cu takes high levels on the actuator for large inclination range. The increase of the inclination causes the detachment of the Cu without changing the purity of the Cu.

Fig. 18 indicates the evolution of the PVC recovery and purity as a function of the inclination angle in the collecting box. The PVC particles are not sensitive to inclination variation. In fact, the recovery rate remains at the same level in the collection box (between 95 and 100 %). However, the purity of PVC particles considerably decreases for inclination beyond 20°. This is explained by a significant effect of gravity on Cu particles at high inclination. Therefore, an inclination angle of 10° is the optimal value that leads to the best separation performance.

Preliminary tests have shown that the charge of the polymer particles acquired by tribo-charging does not affect the separation performance so that the recovery and purity rates remain close to 99 %.

The experimental results show the ability of this separator to exploit the actions of EA actuator on a conductive-insulating mixture.

4. Conclusion

In this work, the effect of an electro-adhesion actuator on a mixture composed on metal/polymer material was investigated and applied for the electrostatic separation of waste electrical cables. The sorting principle consists of attaching the metal particles (Cu) by using the electro-adhesion force on the one hand, and of moving the polymer particles (PVC, PE) mainly by gravity and a mechanical vibration on the other hand. The main results obtained by the two devices developed in this study,

180° rotating system and inclined plane vibrating sorting system, are summarized in the following points:

- Electro-adhesion of Cu particles has been confirmed, particularly when the applied voltage reaches 700 V for a dielectric coating thickness of 27 µm.
- The frequency range that can maintain the EA effect on Cu particles is much wider with a two-phase square signal.
- The action of the electro-adhesion force on the polymer particles is negligible.
- Electrostatic separation of metal/polymer mixtures is possible using an EA actuator inclined up to an angle of 20°; beyond the purity of the recovered materials degrades considerably.
- The optimal configuration for the particles of the studied size range corresponds to the spacing and width electrode ratio K=0.5 and K=1 (equivalent to g = 1 mm, w =1 mm and w = 2 mm).
- High voltage combined with a low angle of inclination makes the electro-adhesive force higher with respect to gravity and mechanical vibration forces.

Obviously, these experiments were preliminary ones and we are well aware that further investigations are necessary to understand more clearly the effect of electrostatic adhesion force on other metal and polymer materials. The present investigation aims at approving the separation technique at a laboratory scale by the electro adhesion method. On a large scale, it would be interesting to adapt the vibrating actuator by a controller system to ensure a continuous operation of the electrostatic sorting process in an industrial application.

Acknowledgement

This work is supported by a Franco-Algerian cooperation program PROFAS B+ between the University of Poitiers (France) and the University of Oran (Algeria).

References

[1] P. O. of the E. Union, WEEE compliance promotion exercise : final report. 26 (2018) 25-62.

[2] M. N. V. Prasad, M. Vithanage, A. Borthakur, Handbook of Electronic Waste Management: International Best Practices and Case Studies. Butterworth-Heinemann. (2019) 207-240.

[3] S. M. Grimes, D. Maguire, Assessment of priorities in critical material recovery from Waste Electrical and Electronic Equipment, Resour Policy. 68 (2020) 101658.

[4] B. Lu, J. Yang, W. Ijomah, W. Wu, G. Zlamparet, Perspectives on reuse of WEEE in China: Lessons from the EU, Resour. Conserv. Recycl. 135 (2018) 83-92.

[5] G. Richard, S. Touhami, T. Zeghloul, L. Dascalescu, Optimization of metals and plastics recovery from electric cable wastes using a plate-type electrostatic separator, Waste Manag. 60 (2017) 112-122.

[6] R. Q. Honaker, N. Singh,B. Govindarajan, Application of dense-medium in an enhanced gravity separator for fine coal cleaning, Miner. Eng. 13 (4) (2000) 415-427.

[7] S. Brunner, P. Fomin, and C. Kargel, Automated sorting of polymer flakes: Fluorescence labeling and development of a measurement system prototype, Waste Manag. 38 (2015) 49-60.

[8] J. L. Ruiz-Herrero, D. Velasco Nieto, A. López-Gil, A. Arranz, A. Fernández, A. Lorenzana, S. Merino, J. Antonio De Saja, M. Á. Rodríguez-Pérez, Mechanical and thermal performance of concrete and mortar cellular materials containing plastic waste, Constr. Build. Mater. 104 (2016) 298-310.

[9] N. Aslan, Modeling and optimization of Multi-Gravity Separator to produce celestite concentrate, Powder Technol. 174 (3) (2007) 127-133.

[10] A. Tilmatine, K. Medles, S.-E. Bendimerad, F. Boukholda, L. Dascalescu, Electrostatic separators of particles: Application to plastic/metal, metal/metal and plastic/plastic mixtures, Waste Manag. 29 (1) (2009) 228-232.

[11] J. S. Chang, A. J. Kelly, J. M. Crowley, A. J. Kelly, J. M. Crowley, Handbook of Electrostatic Processes. CRC Press.(2018) 365-386.

[12] Y. Higashiyama, K. Asano, Recent Progress in Electrostatic Separation Technology, Part. Sci. Technol. 16 (1) (1998) 77-90.

[13] A. Tilmatine, S. Flazi, K. Medles, Y. Ramdani, L. Dascalescu, Séparation électrostatique: complément des procédés mécaniques de recyclage des déchets industriels, J. Electrostat. 61 (1) (2004) 21-30.

[14] H.-S. Jeon, C.-H. Park, B.-G. Cho, J.-K. Park, Separation of PVC and Rubber from Covering Plastics in Communication Cable Scrap by Tribo-Charging, Sep. Sci. Technol. 44 (1) (2009) 190-202.

[15] A. Iuga, L. Calin, V. Neamtu, A. Mihalcioiu, L. Dascalescu, Tribocharging of plastics granulates in a fluidized bed device, J. Electrostat. 63 (6) (2005) 937-942.

[16] H. M. Veit, T. R. Diehl, A. P. Salami, J. S. Rodrigues, A. M. Bernardes, J. A. S. Tenório, Utilization of magnetic and electrostatic separation in the recycling of printed circuit boards scrap, Waste Manag. 25

(1) (2005) 67-74.

[17] H. Louati, A. Tilmatine, R. Ouiddir, A. Alibida, N. Zouzou, New separation technique of metal/polymer granular materials using an electrostatic sorting device, J. Electrostat. 103 (2020) 103410.

[18] S. Masuda, K. Fujibayashi, K. Ishida, H. Inaba, Confinement and transportation of charged aerosol clouds via electric curtain, Electr. Eng. Jpn. 92 (1) (1972) 43-52.

[19] R. P. Krape, Applications study of electroadhesive devices, Nasa report NCR. 1211 (1968) 3–65.

[20] A. Zouaghi, N. Zouzou, L. Dascalescu, Assessment of forces acting on fine particles on a traveling-wave electric field conveyor: Application to powder manipulation, Powder Technol. 343 (2019) 375-382.

[21] A. C. Yen, C. D. Hendricks, A planar electric curtain used as a device for the control and removal of particulate materials, J. Electrostat. 4 (3) (1978) 255-266.

[22] H. Kawamoto, K. Seki, N. Kuromiya, Mechanism of travelling-wave transport of particles, J. Phys. Appl. Phys. 39 (6) (2006) 1249-1256.

[23] H. Kawamoto, Some techniques on electrostatic separation of particle size utilizing electrostatic traveling-wave field, J. Electrostat. 66 (3) (2008) 220-228.

[24] I. Mahi, R. Messafeur, A. Belgacem, Y. Bellebna, H. Louati, A. Tilmatine, New separation method of metal/plastic micronized particles using travelling wave conveyors, Int. J. Environ.75 (5) (2018) 788-799.

[25] A. Tilmatine, A. Alibida, S. Zelmat, H. Louati, Y. Bellebna, F. Miloua, On the attraction force applied on metal pieces in a traveling wave conveyor, J. Electrostat. 96 (2018) 64-68.

[26] A. Belgacem, A. Tilmatine, Y. Bellebna, F. Miloua, N. Zouzou, L. Dascalescu, Experimental analysis of the transport and the separation of plastic and metal micronized particles using travelling waves conveyor, IEEE Trans. Dielectr. Electr. Insul. 25 (2) (2018) 435-440.

[27] A. Hadj Ali, M. E. Zelmat, S. Touhami, S. Louhadj, Y. Benmimoun, H. Louati, A. Tilmatine, Using a vibrating electrical curtain conveyor for separation of plastic/metal particles, Powder Technol. 373 (2020) 267-273.

[28] S. Louhadj, N. Hammadi, S. Touhami, H. Louati, A. Hadjali, I. E. Kimi, A. Tilmatine, Experimental analysis of the attraction force applied on metal particles using a double-side electrical curtain, J. Electrostat. 105 (2020) 103448.

[29] H. Kawamoto, M. Uchiyama, B. L. Cooper, D. S. McKay, Mitigation of lunar dust on solar panels and optical elements utilizing electrostatic traveling-wave, J. Electrostat. 69 (4) (2011) 370-379.

[30] A. Zouaghi, N. Zouzou, Impact of spatial harmonic waves on dielectric particles displacement in standing and traveling wave electric fields, J. Electrostat. 98 (2019) 25-33.

[31] J. Guo, J. Leng, J. Rossiter, Electroadhesion Technologies for Robotics: A Comprehensive Review, IEEE Trans. Robot. 36 (2) (2020) 313-327.

[32] B. F. Seitz, B. Goldberg, N. Doshi, O. Ozcan, D. L. Christensen, E. W. Hawkes, M. R. Cutkosky, R. J. Wood, Bio-inspired mechanisms for inclined locomotion in a legged insect-scale robot, in IEEE International Conference on Robotics and Biomimetics (ROBIO 2014) 791- 796.

[33] J. Germann, M. Dommer, R. Pericet-Camara, D. Floreano, Active Connection Mechanism for Soft Modular Robots, Adv. Robot. 26 (7) (2012) 785-798.

[34] G. J. Monkman, P. M. Taylor, G. J. Farnworth, Principles of electroadhesion in clothing robotics, Int. J. Cloth. Sci. Technol. 1 (3) (1989) 14-20.

[35] Z. Zhang, J. A. Chestney, M. Sarhadi, Characterizing an electrostatic gripping device for the automated handling of non-rigid materials, Proc. Inst. Mech. Eng. Part B J. Eng. Manuf. 215 (1) (2001) 21-36.

[36] H. Prahlad, R. Pelrine, S. Stanford, J. Marlow, R. Kornbluh, Electroadhesive robots—wall climbing robots enabled by a novel, robust, and electrically controllable adhesion technology, in IEEE International Conference on Robotics and Automation. (2008) 3028-3033.

[37] J. Guo, T. Bamber, M. Chamberlain, L. Justham, M. Jackson, Optimization and experimental verification of coplanar interdigital electroadhesives, J. Phys. D: Appl. Phys. 49 (41) (2016) 415304.

[38] J. Mao, L. Qin, Y. Wang, J. Liu, L. Xue, Modeling and simulation of electrostatic attraction force for climbing robots on the conductive wall material, in IEEE International Conference on Mechatronics and Automation. (2014) 987-992.

[39] R. Chen, Y. Huang, Q. Tang, An analytical model for electrostatic adhesive dynamics on dielectric substrates, J. Adhes. Sci. Technol. 31 (11) (2017) 1229-1250.

[40] R. Chen, Z. Zhang, R. Song, C. Fang, D. Sindersberger, G. J. Monkman and J. Guo, Time-dependent electroadhesive force degradation, Smart Mater. Struct. 29 (5) (2020) 055009.

[41] T. Nakamura, A. Yamamoto, Modeling and control of electroadhesion force in DC voltage,Robomech J. 4 (18) (2017).

[42] C. Cao, X. Sun, Y. Fang, Q.-H. Qin, A. Yu, and X.-Q. Feng, Theoretical model and design of electroadhesive pad with interdigitated electrodes, Mater. Des. 89 (2016) 485-491.

[43] J. Fessl, F. Mach, and J. Navrátil, Design, fabrication and testing of electroadhesive interdigital electrodes, Open Phys. 16 (1) (2018) 430-434.

[44] S. M. J. Mahmoudzadeh Akherat, M. A. Karimi, V. Alizadehyazdi, S. Asalzadeh, M. Spenko, A tunable dielectric to improve electrostatic adhesion in electrostatic/microstructured adhesives, J. Electrost. 97 (2019) 58-70.

[45] A. Yamamoto, T. Nakashima, T. Higuchi, Wall Climbing Mechanisms Using Electrostatic Attraction Generated by Flexible Electrodes, in International Symposium on Micro-Nano Mechatronics and Human Science, Nagoya, Japan, (2007) 389-394.

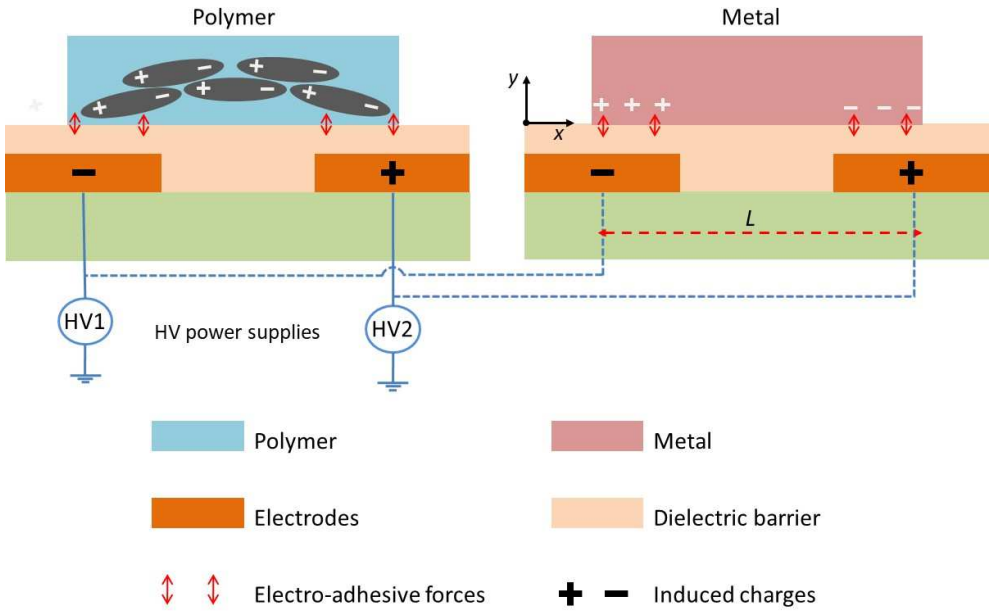

Fig. 1. Schematic illustration of EA actuator principle for polymer and metal materials

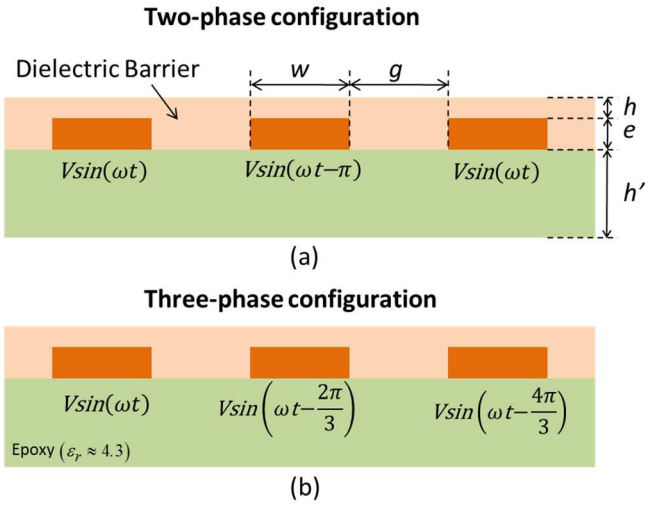

Fig. 2. Schematic illustration of the EA actuators. Dimensions of the reference actuator: $w = g = 1\ mm$, $h = 0.027\ mm$, $e = 0.035\ mm$, and $h' = 1.5\ mm$.

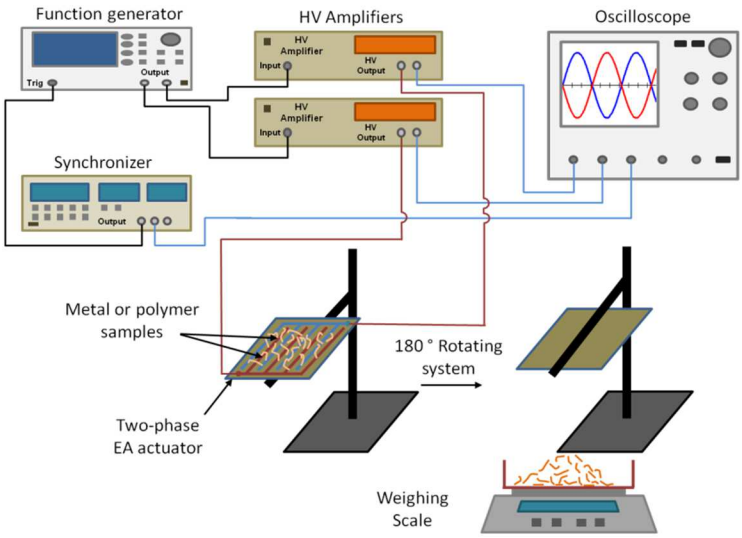

(a)

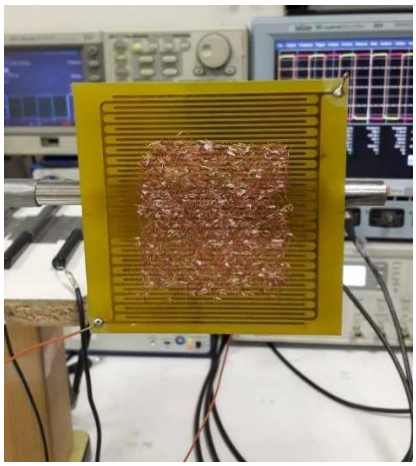

(b)

Fig. 3. 180 ° rotating system. (a) Schematic illustration. (b) Photography of copper samples attached on an EA actuator turned on and positioned in a vertical position.

(a) (b) (c)

Fig. 4. Photography of particle samples. (a) Cu. (b) PE. (c) PVC.

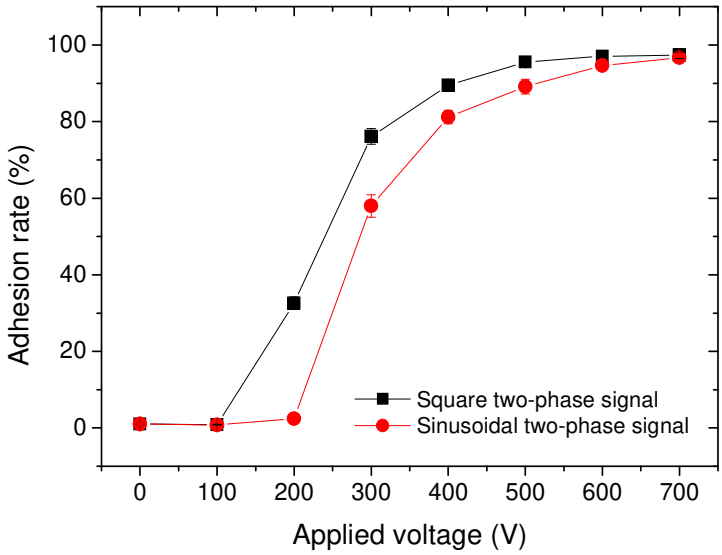

Fig. 5. Variation of the copper adhesion rate as a function of the applied voltage for square and sinusoidal two-phase signals. Conditions: $f = 300\ Hz$, $g = w = 1\ mm$.

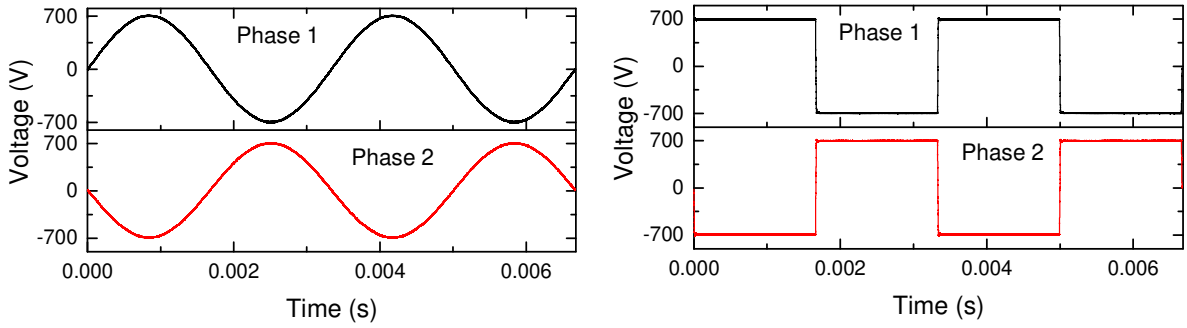

(a) (b)

Fig. 6. Typical experimental waveforms of the applied voltage used for the two-phase actuator (a) sine and (b) square signals. Conditions: $V_{max} = 700\,V$, $f = 300\,Hz$.

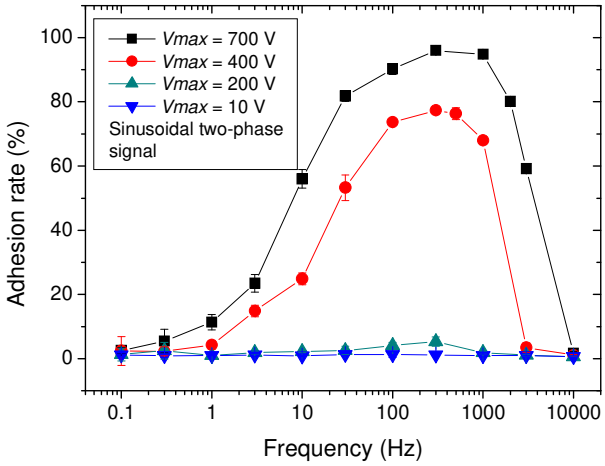

Fig. 7. Variation of the Cu adhesion rate as a function of the frequency in the case of a sinusoidal two-phase signal. Conditions: $g = w = 1\,mm$.

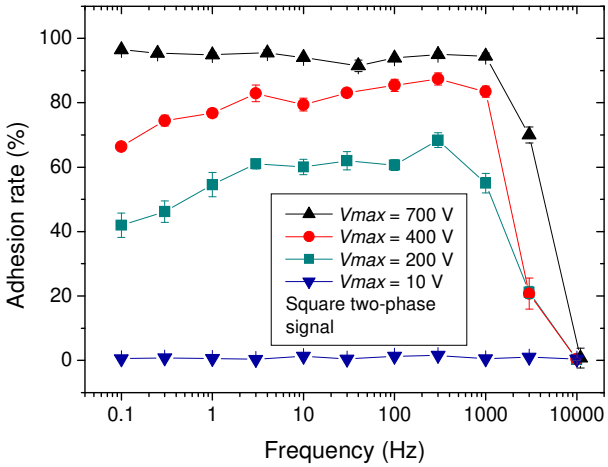

Fig. 8. Variation of the Cu adhesion rate as a function of the frequency in the case of a square two-phase signal. Conditions: $g = w = 1\ mm$.

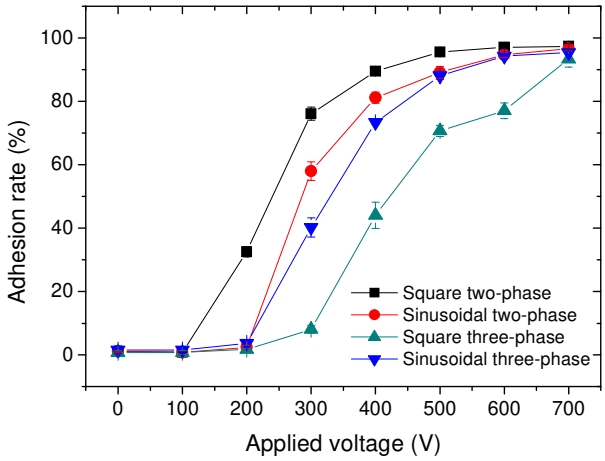

Fig. 9. Influence of the signal type and the electrodes distribution on the Cu adhesion rate as a function of the applied voltage. Conditions: $f = 300\ Hz$, $g = w = 1\ mm$.

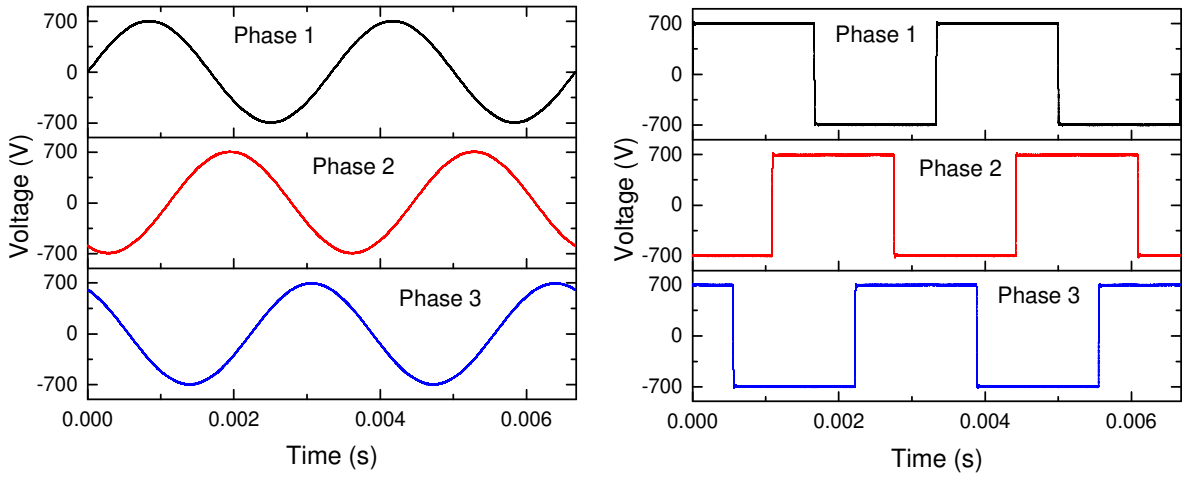

Fig. 10. Typical experimental voltage waveforms for the tree-phase actuator (a) sine and (b) square signals. Conditions: $V_{max} = 700\,V$, $f = 300\,Hz$, and $g = w = 1\,mm$.

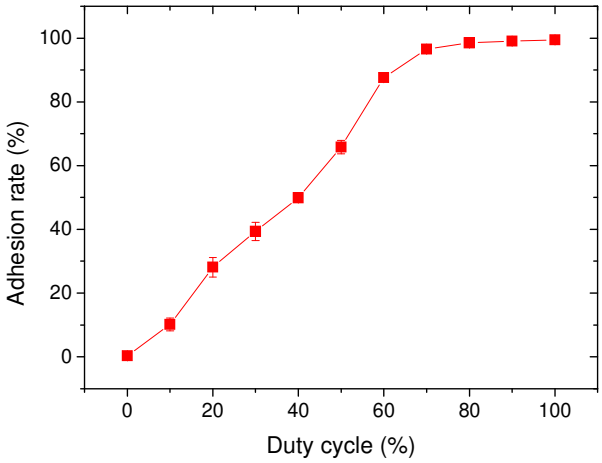

Fig. 11. Evolution of Cu adhesion rate as a function of the duty cycle for a square two-phase signal.

Conditions: $V_{max} = 700\ V$, $f = 300\ Hz$, and $g = w = 1\ mm$.

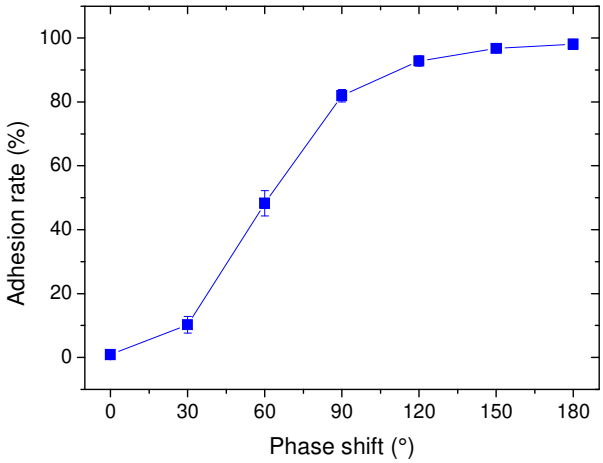

Fig. 12. Evolution of Cu adhesion rate as a function of the phase shift for a square two-phase signal.

Conditions: $V_{max} = 700\ V$, $f = 300\ Hz$, and $g = w = 1\ mm$.

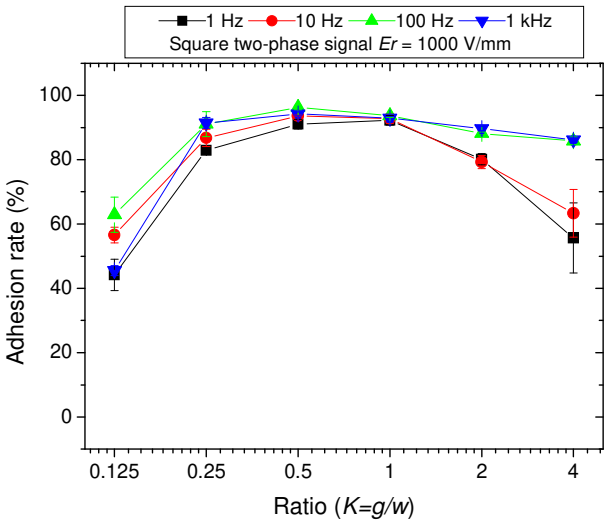

Fig. 13. Evolution of Cu adhesion rate as a function of g/w ratio for different frequencies

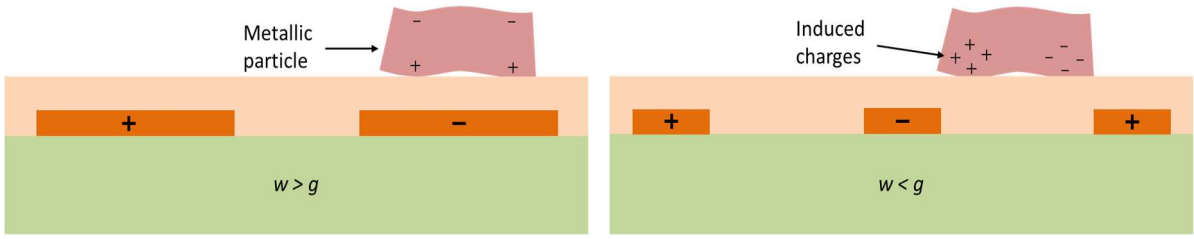

Fig. 14. Schematic representation of possible particle position on the actuator for: (a) high electrode width and (b) high gap.

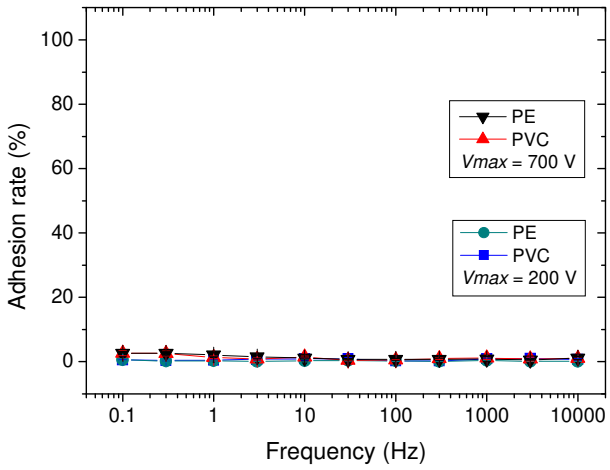

Fig. 15. Evolution of the adhesion rate of PE particles as a function of frequency in the case of a square two-phase signal at 200 V and 700 V ($g = w = 1\,mm$).

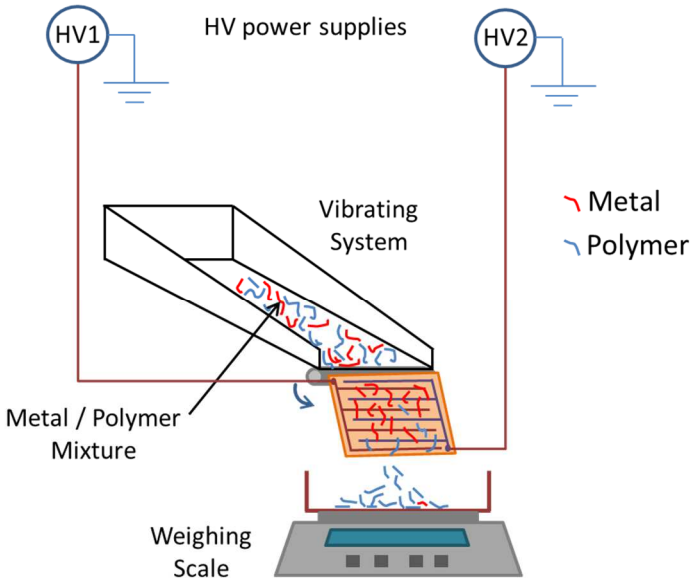

(a)

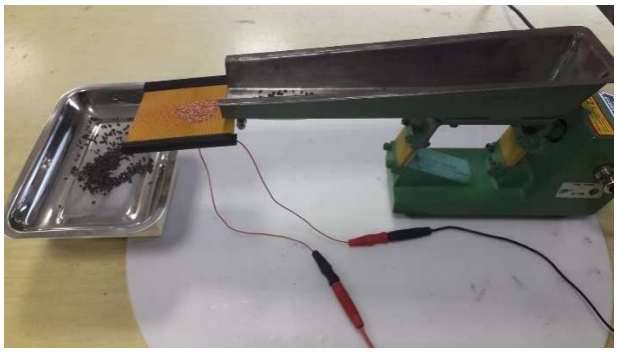

(b)

Fig. 16. Inclined plane vibrating sorting system of Cu / PVC mixture: (a) schematic illustration, (b) photography of the electrostatic sorting operation.

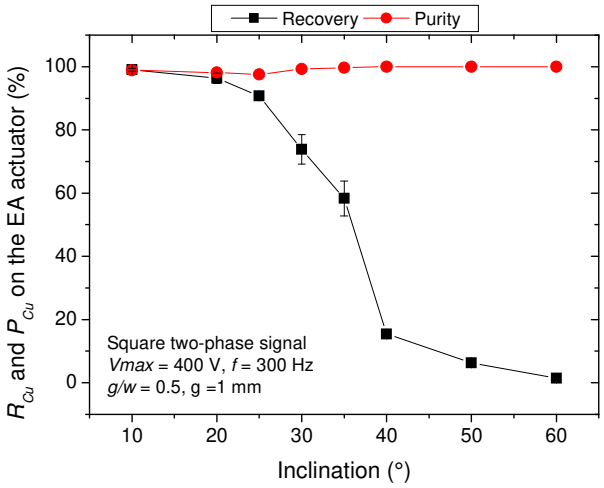

Fig. 17. Recovery and purity of Cu on the EA actuator surface as a function of the inclination angle.

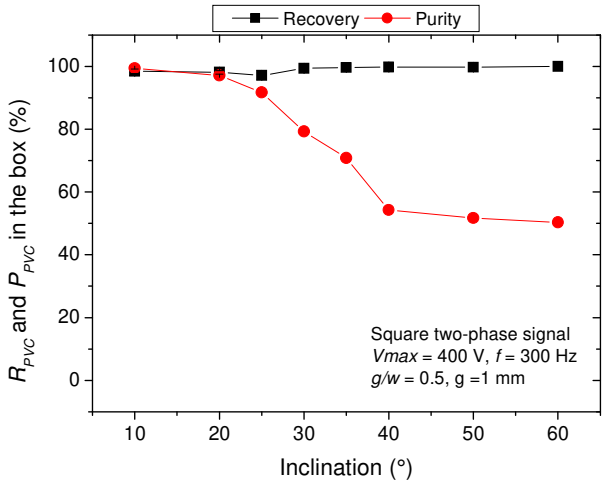

Fig. 18. Recovery and purity of PVC in collection box as a function of the inclination degree.

Table 1. The electrode width w and spacing g for the used actuators (K=1 corresponds to reference case)

g (mm)	w (mm)	$K = g/w$
0.5	4	0.125
1	4	0.25
1	2	0.5
1	1	1
2	1	2
4	1	4

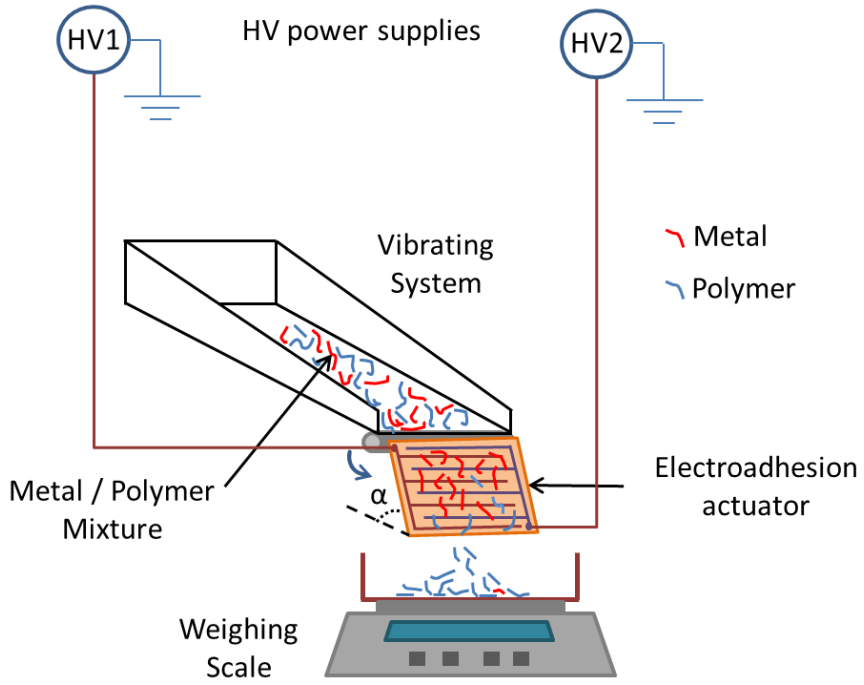

Device for electrostatic sorting of metal/polymer particle mixture

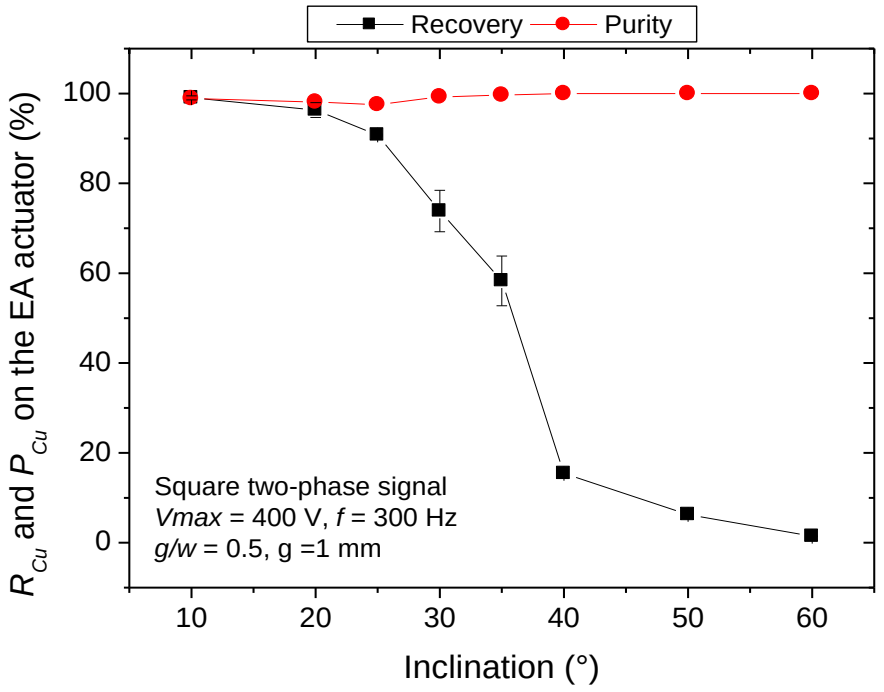

Typical results of copper recovery and purity as a function of inclination angle